Effects of blackbody radiation on highly excited atoms

W. E. Cooke

Department of Physics, University of Southern California, University Park, Los Angeles, California 90007

T. F. Gallagher

Molecular Physics Laboratory, SRI International, Menlo Park, California 94025

Transitions between energetically close-lying Rydberg states are characterized by large electric dipole matrix elements and frequencies low enough that at room temperature the photon occupation number is $\simeq 10$. Consequently the absorption of blackbody radiation and the stimulated emission produced by it lead to an efficient redistribution of population among nearby levels. In some cases dramatic effects are observed, for example, radiative lifetimes that are shortened to a small fraction of their $T = 0$ values. In addition, the 300-K blackbody field of ~ 10 V/cm produces ac Stark shifts of the Rydberg levels. Calculations of the population redistribution effects and ac Stark shifts are presented. Examples are given to illustrate that care must be taken in experiments with highly excited atoms to ensure that only one state is being observed rather than a distribution.

I. INTRODUCTION

Previously[1,2] it has been noted that room-temperature blackbody radiation can both produce a rapid redistribution of Rydberg-state population by stimulated emission and absorption as well as ac frequency shifts. We described a specific example of the former effect, the threefold reduction of the Na $17p$ and $18p$ lifetimes by blackbody-induced stimulated emission and absorption. Here we present a more detailed and expanded description of both the blackbody-induced transition rates and the ac Stark effects for Rydberg states. We also present in detail two examples to illustrate how the population redistribution effects enter into different classes of Rydberg-atom experiments.

II. RADIATIVE LIFETIMES AND ac STARK SHIFTS

The usual expression for the radiative lifetime τ_n of state n is given by the oscillator strength sum[3]

$$1/\tau_n = -2\alpha^3 \sum_{n'} \omega_{nn'}^2 f_{nn'} , \qquad (1a)$$

$$f_{nn'} = \tfrac{2}{3}\omega_{n'n} r_{nn'}^2 \, g_>/(2g_n+1) , \qquad (1b)$$

$$\omega_{nn'} = W_n - W_{n'} , \qquad (1c)$$

where the sum in Eq. (1a) is only over lower states n', such that $W_{n'} < W_n$, making the oscillator strength $f_{nn'}$ negative. All three equations are in atomic units, where α is the fine-structure constant, W_n is the energy of state n, g_n is the de-

generacy of state n, $g_>$ is the larger of g_n and $g_{n'}$, and $r_{nn'}^2$ is the square of the radial matrix element of r between states n and n'. However, if $T \neq 0$, then blackbody radiation will cause transitions through both stimulated emission and absorption. This will produce an additional decay term[4]

$$1/\tau_n^b = 2\alpha^3 \sum_{n'} \bar{n}_\omega \omega_{nn'}^2 |f_{nn'}| , \qquad (2)$$

where $\bar{n}_\omega$ is the occupation number for photons of frequency $|\omega_{nn'}|$. In Eq. (2), the sum is now extended over all values of n'.

It is useful to derive an approximate expression for Eq. (2) both to show clearly systematic the n and l dependence of τ_n^b and to provide a simple alternative to the cumbersome sum of Eq. (2). For Rydberg states, most states n' are nearby in energy, so that $\bar{n}_\omega$ may be approximated by $|kT/\omega|$, which is valid for $\bar{n}_\omega > 1$. Then Eq. (2) may be written

$$1/\tau_n^b = 2\alpha^3 kT \sum_{n'} \omega_{n'n} f_{nn'} . \qquad (3)$$

But the sum over oscillator strengths satisfies a sum rule[3]:

$$\sum \omega_{n'n} f_{nn'} = \tfrac{4}{3}(W_n - \bar{V}_n) = 2/3n^{*2} , \qquad (4)$$

where $\bar{V}_n$ is the average value of the potential energy (equal to $1/n^{*2}$ for hydrogenlike atoms such as Rydberg states). Thus for T in degrees Kelvin, the additional rate due to blackbody-stimulated transitions is

$$1/\tau_n^b = 4\alpha^3 kT/3n^{*2} = 6.79 \times 10^4 (T/n^{*2}\,\text{sec}^{-1}\,.$$

$$(5)$$

At room temperature this is a rate of 6.9 $\times 10^4\,\text{sec}^{-1}$ for a Na $18p$ state. One should note that this rate is independent of l and of the atomic species (except for the small variations in n^*). Of particular interest are the high-l states, for which the radiative lifetimes are long, and the blackbody-induced transitions are thus the dominant decay mechanism. In this case the transitions will necessarily be to other long-lived high-l states so that the total Rydberg population will still appear to be long lived, but Eq. (5) puts a fundamental limit on the time during which a "pure" Rydberg-nl-state population can be maintained.

The only approximation used in obtaining Eq. (5) was $\bar{n}_\omega \simeq |kT/\omega|$, which is an overestimation of $\bar{n}_\omega$ for large ω [since eventually $\bar{n}_\omega \simeq \exp(-\omega/kT)$]. Thus Eq. (5) is an upper limit to $1/\tau_n^b$, the error reflecting the extent to which $\bar{n}_\omega \neq kT/\omega$. As n increases, Eq. (5) becomes increasingly more accurate because the strongest transitions lie at lower frequencies for which $\bar{n}_\omega = kT/\omega$ is valid. To provide a quantitative feeling for this, we have evaluated Eqs. (2) and (5) for several Na states. Using the Bates-Damgaard[5] method to calculate the radial matrix elements we may evaluate Eq. (2) for the 11s and 21s ($n^* = 9.65$ and 19.65) states, obtaining rates of $9.78 \times 10^4\,\text{sec}^{-1}$ and $3.53 \times 10^4\,\text{sec}^{-1}$ whereas Eq. (5) yields rates of $2.08 \times 10^5\,\text{sec}^{-1}$ and $5.25 \times 10^4\,\text{sec}^{-1}$, values which are 113 and 49% too high. In both cases, the errors are presumably due to the high-frequency transitions to lower-lying states for which $\bar{n}_\omega \ll 1$. Thus the errors for the 11s and 21s states, 1.30×10^5 and $1.73 \times 10^4\,\text{sec}^{-1}$, respectively, should be considerably smaller than the radiative decay rates, obtained from Eq. (2) with $n_\omega = 1$, and in fact they are. The 11s and 21s radiative decay rates are 8.0×10^5 and 9.5×10^4 sec^{-1}, respectively.[6]

Not surprisingly, as l is increased, Eq. (5) also becomes more accurate, since there are no longer available high-frequency transitions to low-lying states. For example, for the highest l states of $n = 15$ and $n = 20$, Eq. (2) yields rates of 7.57×10^4 and $4.77 \times 10^4\,\text{sec}^{-1}$, whereas Eq. (5) yields rates of 9.17×10^4 and $5.10 \times 10^4\,\text{sec}^{-1}$, which are 21% and 6% too high. Thus Eq. (5) is a most accurate estimate for the high-l states that are most affected by the redistribution effect.

Oscillator strength sums may also be used to calculate ac Stark shifts induced by blackbody radiation. The ac Stark shifts, however, are primarily due to the electric field components near the frequency of peak blackbody intensity, $\sim 3kT$. These frequencies are thus usually far off resonance and result in an energy shift[7]:

$$\Delta W \sum_{n'} \frac{|\mu_{nn'}|^2 E_b^2\,\omega_{nn'}}{2(\omega_{nn'}^2 - \omega_b^2)} \simeq \frac{1}{4}\frac{E_b^2}{\omega_b^2}\sum_{n'} f_{nn'} = \frac{1}{4}\frac{E_b^2}{\omega_b^2}\,,$$

$$(6)$$

where $\mu_{nn'}$ is the dipole matrix element between states n and n', E_b is the electric field due to blackbody radiation at frequency ω_b, and we have used the approximation $\omega_b \gg \omega_{nn'}$. Note that Eq. (6b) shows the same shift as it would for a free electron, so that we have the not-surprising result that a highly excited state responds to a high-frequency electric field just as a free electron does.

However, for blackbody radiation, the electric field E_b due to radiation in a bandwidth $d\omega$ is[4]

$$E_b^2 = \frac{8\omega^3\alpha^3}{\pi}\frac{d\omega}{\exp(\omega/kT) - 1}\quad (\text{in a.u.})\,.\quad (7)$$

This may be substituted into Eq. (6) and integrated to obtain

$$\Delta W = \tfrac{1}{3}\pi\alpha^3(kT)^2\,.\qquad (8)$$

For $T = 300$ K, this shift is 2.2 kHz, independent of n, l, and the atomic species. Thus it can only be observed in transitions from low-lying states which are not affected by E_b^2 (since $\omega_b < \omega_{nn'}$ for those states).

It is expected that Eq. (8) will be more accurate than Eq. (5) was, since the sum is only over oscillator strengths, rather than the products of frequencies and oscillator strengths. Typically the oscillator strength will be maximum for adjacent transitions ($|f_{n,n\pm1}| \simeq (1/n^*)^3 \ll \omega_b$), and decline rapidly to $\sim 1/n^{*3}$ for large-ω transitions. Since the integral over frequencies did include some terms where $\omega_b < \omega_{nn'}$, Eq. (8) overestimates the shift by a fractional amount of the order $10^5/[T(n^*)^3]$ for T in degrees Kelvin.

Since the power spectrum of blackbody radiation changes relatively slowly with frequency, shifts due to near resonant terms will in general cancel, thus allowing the substitution of ω_b^2 for $\omega_{nn'}^2 - \omega_b^2$ in Eq. (6a). By numerically integrating over the blackbody power density, we have determined that this substitution introduces an error of less than 0.3 (ω_{nn}'/kT) for values of ω_{nn}' up to $\tfrac{1}{2}kT$. Again, since the largest contributions to Eq. (6b) come from nearby states, Eq. (8) has an uncertainty of order $0.3/(n^3 kT) \simeq 300/n^3$ at room temperature.

Previously we pointed out that the rate at which the 300-K blackbody-induced transitions depopu-

late Rydberg states is comparable to the collisional depopulation rate produced by 10 mtorr of Ar (using an estimated cross section of 20 Å^2 for Na-ns-state depopulation by Ar). Thus the effect of the blackbody radiation is analogous to pressure broadening. Similarly the blackbody ac Stark effect which shifts all the Rydberg levels together is analogous to the pressure shifts induced in Rydberg states by rare gases. That is a series of high-n ($n > 10$) states all have the same pressure shift.[8] This has been observed by direct measurement of pressure shifts in the optical absorption from the ground state[8] and can be inferred from the absence of collisional dephasing arising from differential pressure shifts between Rydberg levels.[9] Thus it appears that the blackbody photons behave like foreign gas atoms in both the shifts and broadenings they produce in Rydberg atoms.

III. IMPLICATIONS OF POPULATION REDISTRIBUTION FOR EXPERIMENTS WITH RYDBERG ATOMS

While the effect of blackbody radiation of the radiative lifetimes can be very dramatic, it is the rapid diffusion of population from an initially excited Rydberg state to other nearby states which is of general importance for experiments with Rydberg atoms. We can get a feeling for the magnitude of the effect by considering a specific example, the Na 18s state. The thermal bath of photons transfers population from the 18s state to the two neighboring p states at a rate of 4×10^4 sec^{-1}, while the radiative decay rate[6] is only 1.6×10^5 sec^{-1}. Thus roughly a quarter of the initial population can become redistributed over nearby Rydberg states!

To illustrate how the population redistribution effects affect different types of measurements, we discuss here how they affect field-ionization-

threshold measurements and radiative-lifetime measurements using selective field ionization (SFI).

The experimental approach and apparatus have been described in detail elsewhere[10] so we shall only outline them briefly here. In the experiment we pass an atomic beam of Na between a plate and a grid 1.12 cm apart where it is crossed by two 5-nsec dye-laser pulses which excite, for example, the $3s \to 3p$ and $3p \to 18s$ transitions as shown in Fig. 1. At a variable time after the laser excitation we apply a positive high-voltage pulse (up to 10 kV) to the plate ionizing the Rydberg atoms and accelerating the ions formed through the grid into a particle multiplier. By varying the amplitude of the ionizing pulse we can selectively ionize specific excited states (field-ionization thresholds for the states of interest are given in Ref. 8). Thus we are able to determine the time evolution of the population of each state after the laser pulse.

The characterization of electric field ionization thresholds is typically done by applying a pulsed field to the Rydberg atoms after the laser excitation.[10-12] In the absence of blackbody radiation the time delay between excitation and ionization would make no difference in the measurement of the field-ionization threshold [although it would lead to very small (1%) signals at higher thresholds due to radiative decay to nearby lower states]. However, in previous work[10,12] where the delays were 0.5–1.0 μsec, the signal for a field 10–20% below threshold was $\simeq 5\%$ of the signal above threshold. In Fig. 2 we show an example of this, the field-ionization threshold of the Na 18s state obtained after a delay of $\simeq 1$ μsec between the laser excitation and field-ionization pulse. The 18s threshold at 4.40 kV/cm is apparent, and it is also clear that even for fields as low as 4.2 kV/cm that the ionization signal is
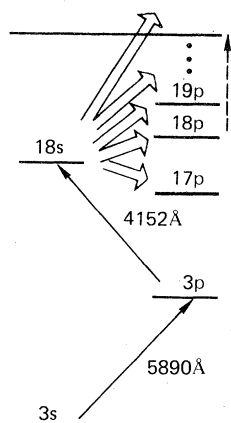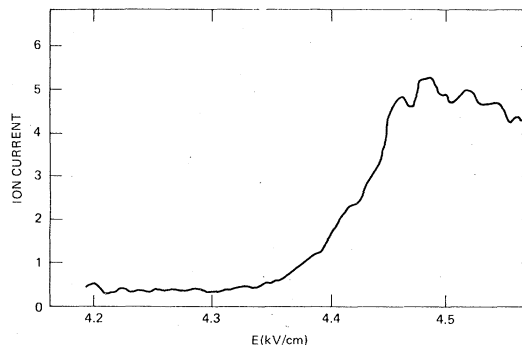

FIG. 1. Relevant energy levels for the experiment with the Na 18s state. Solid vertical arrows indicate laser excitation, double arrows indicate blackbody excitation, and the broken arrow indicates field ionization (shown for the 18s state).

FIG. 2. Field-ionization threshold for the Na 18s state with the ionization pulse delayed by $\simeq 1$ μsec from the laser excitation. Note that the signal below the threshold is $\simeq 5\%$ of the signal above threshold.

$\simeq 5\%$ of the signal above the ionization threshold. Since the field-ionization rate for a field 10% below threshold should be reduced by three orders of magnitude[13] a 5% ionization signal is a somewhat puzzling result. This discrepancy has been ascribed to a nonselective field-ionization[12] effect or photoionization[14] while related effects in high electric fields have been attributed to collisional ionization.[15] In fact both of these effects are probably due to the blackbody flux acting after the laser excitation. We have tested this hypothesis by investigating several aspects of the field ionization of the initially excited Na 18s state. First, we measured the ionization produced by several values of fields below the threshold field of 4.40 kV/cm as a function of time after the laser excitation. Owing to the 0.6-μsec rise time of our ionization pulse, we were forced to extrapolate to $t = 0$. In Fig. 3 we show the observed ionization signals expressed as a percentage of the 18s-state signal observed above threshold as a function of t for various values of ionizing field. As shown by Fig. 3 all the signals extrapolate back to a nonzero signal, which is due to photoionization of the Na 3p state by dye-laser fluorescence at $\lambda < 4084$ Å. This signal persists when the second laser is detuned from the 3p-18s transition.

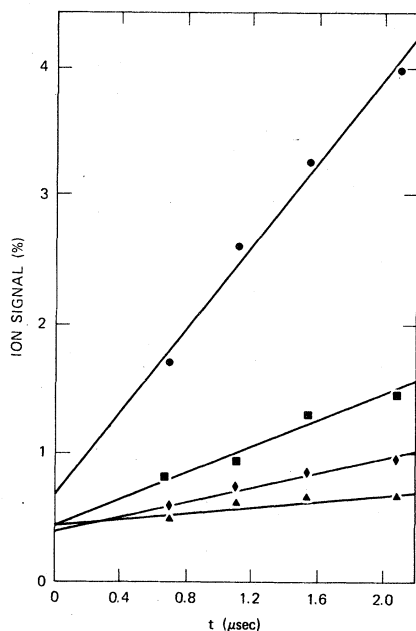From Fig. 3 we can see that for fields of 3.25 kV/cm or less, 25% or more below the 18s

FIG. 3. Fraction of the initial Na 18s population ionized by electric fields below the 18s ionization threshold vs time between excitation and ionization for ionizing fields of 4.14 (●), 3.25 (■), 2.22 (♦), and 1.38 kV/cm (▲).

threshold the ionization signal at $t = 0$ is reduced by at least a factor of 3×10^3. For a field of $\simeq 6\%$ below the ionization threshold half point ($\simeq 8\%$ below the 90% point) we see a signal which is 0.3% of the signal above threshold. This can be compared with the calculations of Bailey et al.,[13] which show an order-of-magnitude increase in ionization rate for each 3% increase in field, implying a factor of $\simeq 300$ difference between the ionization fields at $E = 4.14$ and $E > 4.50$ kV/cm, as observed. Our previous ionization measurements corresponded to $t \simeq 1$ μsec on Fig. 3, making it clear why we only saw increases of a factor of 20 when the field was raised from 10% below threshold to above threshold.

The difference in the ionization signals for the different field values shown in Fig. 3 implies that the ionization signal below the threshold field has a field dependence. In fact, if our hypothesis that this signal is due to black body-induced transitions to higher-lying p states is correct, the signal should not increase gradually with ionizing field but should exhibit thresholds corresponding to 18p, 19p, etc. To check this we delayed the ionization pulse 4 μsec and scanned the ionizing field as shown in Fig. 4. As shown by Fig. 4 in the field range from 3.4 to 4.0 kV/cm, we do not see a gradual increase in the signal but a clear threshold at 3.65 kV/cm corresponding to the 18p state.

To ensure that the signals of Figs. 4 and 5(b) were not collisionally induced, we observed the ratio of populations in the 18s and higher-lying states at $t = 5$ μsec while systematically varying the background pressure, atomic beam density, and laser power. We varied the pressure from 8×10^{-7} to 4×10^{-5} torr using argon and air, the atomic beam density was varied in order of magnitude above and below the normal operating point of 10^9 cm^{-3}, and both laser intensities were varied a factor of at least 5 above and below the normal level. In all cases the observed variation of the 18s/18p ratio was < 10%. Thus at our typical operating conditions we estimate that all of the collision processes taken together contribute at most 3% to the observed signal at ionizing fields less than 4.40 kV/cm [Fig. 5(b)]. We are thus reasonably confident that the signals observed at fields below the ionization fields do come from blackbody-induced transitions to higher-lying states.

Although this effect is in general a disadvantage, we can use it to our advantage because it allows us to detect, by field ionization, states which we are not able to field ionize directly. Specifically, if immediately after the laser pulse we try to field ionize excited states of $n < 15$ we are unable to de-
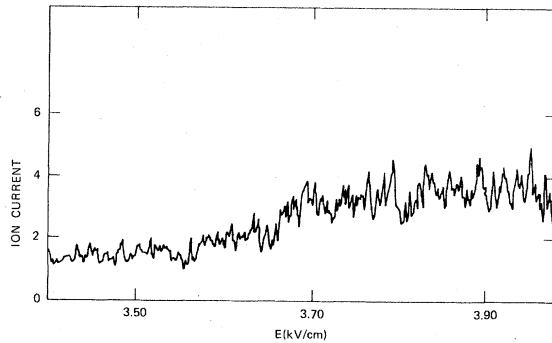
FIG. 4. Ionization signal vs peak ionizing field when the Na 18s state is initially populated. The ionizing field is applied 4 μsec after the laser excitation and shows a pronounced threshold at 3.65 kV/cm, which is due to blackbody-induced transitions at the 18s state. The 18s ionization threshold is at 4.40 kV/cm. The absolute accuracy of the electric field measurement is ≃ 6%.

tect them with our ionizing fields of 10 kV/cm. However, if we wait 3 μsec, after the laser excitation we are able to detect ionization from initially excited states as low as $n = 10$ using fields of 1 kV/cm, implying that the blackbody radiation has excited some of the atoms to states of $n > 24$ or into the continuum during the 3 μsec delay. A similar effect may be responsible for the observation of Xe states down to $n = 8$ rather than laser photoionization.[12]

The measurement of radiative lifetimes using SFI requires particular care. In the absence of blackbody radiation the 18s state only decays via spontaneous emission to lower states and a negligible fraction, ≃1%, of the atoms decay to the 17p state. To measure the 18s lifetime, then, a reasonable approach would be to set the amplitude of the ionizing pulse slightly above the 18s threshold, 4.40 kV/cm, and record the ion signal
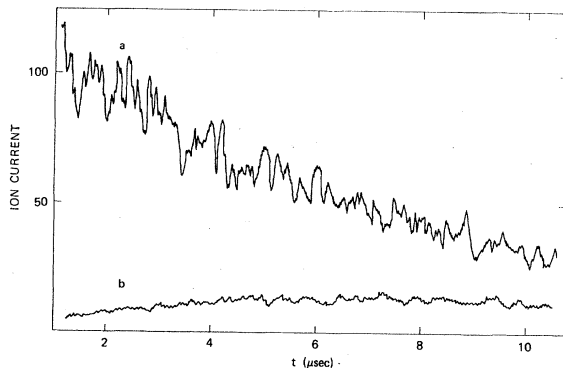

FIG. 5. Observed time dependence of the ionization signal following the initial population of Na 18s state with an ionizing field of (a) 4.85 and (b) 4.14 kV/cm.

as a function of the time t between the laser pulse and the ionizing pulse. Figure 5 is just such a scan with an ionization field of 4.85 kV/cm, yielding a decay time of 7.8 μsec. However, we know that the blackbody radiation will excite transitions from the 18s state to nearby higher- and lower-p states at appreciable rates. Since the ionization pulse of Fig. 5 is in fact above both of the 17p thresholds of 4.44 and 4.70 kV/cm. Figure 5 represents the population in the 17p state and all higher states. We can easily tell what fraction of the signal of Fig. 5(a) is due to states higher than 18s by reducing the ionizing pulse to 4.14 kV/cm. yielding Fig. 5(b). If we investigate the threshold behavior of the signal at $t = 5$ μsec, we can identify the states contributing to Fig. 5(b). We find a pronounced threshold at 3.65 kV/cm, corresponding to the 18p state, and less-clear thresholds at 2.95 and 2.40 kV/cm corresponding to the 19p and 20p states, respectively. By measuring the signal at $t = 5$ μsec as a function of ionizing field we determined that 60% of the signal of Fig. 5 is due to the 18p state. We calculate the total transition rates for the transitions $18s \rightarrow 17p$ and $18s \rightarrow 18p$ to be 2.14×10^4 and 2.28×10^4 sec^{-1}, respectively. Using this we know that the 17p component of Fig. 5(a) is equal to 56% of Fig. 5(b). Thus the 18s population $N(t)$ is given by

$$N(t) = A(t) - 1.56 \, B(t) , \qquad (9)$$

where $A(t)$ and $B(t)$ are the magnitudes of the signals of Figs. 5(a) and 5(b), respectively. From Eq. (9) we determine the measured value of the 18s lifetime τ^* to be 4.78 μsec. The radiative lifetime τ of the 18s state is calculated by Gounand[6] to be 6.37 μsec. With the calculated τ^b of 35.0 μsec, we find $\tau^* = 4.87$ μsec, in excellent agreement with the experimental results. Note that the decay time of 7.8 μsec obtained ignoring blackbody radiation is in error by almost a factor of 2! The systematic checks described above ensured that the signal of Fig. 5(b) was not collisionally induced.

IV. CONCLUSIONS

Here we have illustrated the importance of blackbody radiation for Rydberg-atom studies by several experiments conducted at 300 K. In fact, it would be interesting to study these effects as a function of temperature but it is nonetheless clear that the presence of blackbody radiation must be considered in any investigation of Rydberg-atom properties. Most important is the fact that the initial excitation becomes diffused among nearby states at substantial rates. (At high excitation

densities it can even induce super-radiance.[16])
The high blackbody transition rates at 300 K could completely obscure, for example, the low collision rate of a crossed-beam experiment (low temperatures will be required for such experiments). Even if the blackbody radiation does not make such an experiment impossible, it will certainly lead to a distribution of states which must be taken into account in the analysis of the data.

[1] T. F. Gallagher and W. E. Cooke, Phys. Rev. Lett. 42, 835 (1979).

[2] E. J. Beiting, G. F. Hildebrandt, F. G. Kellert, G. W. Foltz, K. A. Smith, F. B. Dunning, and R. F. Stebbings, J. Chem. Phys. 70, 3551 (1979).

[3] H. A. Bethe and E. A. Salpeter, The Quantum Mechanics of One and Two Electron Atoms (Academic, New York, 1957).

[4] R. Loudon, The Quantum Theory of Light (Oxford University, London, 1973).

[5] D. R. Bates and A. Damgaard, Philos. Trans. R. Soc. London 242, 101 (1949).

[6] F. Gounand (unpublished).

[7] C. H. Townes and A. L. Schawlow, Microwave Spectroscopy (McGraw-Hill, New York, 1955).

[8] E. Amaldi and E. Segre, Nuovo Cimento 11, 145 (1934).

[9] T. F. Gallagher and W. E. Cooke, Phys. Rev. A 19, 2161 (1979).

[10] T. F. Gallagher, L. M. Humphrey, W. E. Cooke, R. M. Hill, and S. A. Edelstein, Phys. Rev. A 16, 1098 (1977).

[11] T. W. Ducas, M. G. Littman, R. R. Freeman, and D. Kleppner, Phys. Rev. Lett. 35, 366 (1975).

[12] R. F. Stebbings, C. J. Latimer, W. P. West, F. B. Dunning, and T. B. Cook, Phys. Rev. A 12, 1453 (1975).

[13] D. S. Bailey, J. R. Hiskes, and A. C. Riviere, Nucl. Fusion 5, 41 (1965).

[14] T. F. Gallagher, W. E. Cooke, and S. A. Edelstein, Phys. Rev. A 17, 904 (1978).

[15] M. G. Littman, M. L. Zimmerman, and D. Kleppner, Phys. Rev. Lett. 37, 486 (1976).

[16] W. E. Cooke and T. F. Gallagher (unpublished).